Available online at www.sciencedirect.com
SCIENCE DIRECT®
Journal of Organometallic Chemistry 690 (2005) 802–810
Journal of Organometallic Chemistry
www.elsevier.com/locate/jorganchem

Synthesis, NMR, IR spectroscopic and X-ray study of novel [pyridazin-3(2H)-one-6-yl]ferrocenes and related ferrocenophane derivatives. Study on ferrocenes. Part 14 ☆

Antal Csámpai [a], Árvácska Abrán [a], Veronika Kudar [a], György Túrós [a], Heinrich Wamhoff [b], Pál Sohár [a,*]

[a] *Research Group for Structural Chemistry and Spectroscopy, Hungarian Academy of Sciences – Department of General and Inorganic Chemistry, Eötvös Loránd University, P.O. Box 32, H-1518 Budapest, Hungary*

[b] *Kekulé Institut für Organische Chemie und Biochemie der Universität Bonn, Gerhard-Domagk Str. 1, D-53121 Bonn, Germany*

Received 27 May 2004; accepted 9 September 2004

Abstract

On treatment with glyoxylic acid and hydrazine hydrate, 1,1′-diacetylferrocene was converted into the separable mixture of 1,1′-*bis* [pyridazin-3(2*H*)-one-6-yl]ferrocene and the hydrazone as well as the azine of 1-acetyl-1′-[pyridazin-3(2*H*)-one-6-yl]ferrocene. Successful cyclizations of 1,1′-*bis*[pyridazin-3(2*H*)-one-6-yl]ferrocene resulting in a series of novel ferrocenophanes containing heterocyclic units were performed under phase transfer- and homogeneous catalytic (RCM) conditions by the application of versatile dialkylating agents and second generation Grubbs' catalyst, respectively. The structures were determined by mass spectrometry, IR, ^{1}H and ^{13}C NMR spectroscopy including 2D-COSY, HMQC and HMBC measurements. The solid phase structure of a dimer product with π-stacking interaction was revealed by X-ray analysis.

Keywords: Ferrocene; Pyridazine; Phase transfer reaction; Ring closing metathesis; π-Stacking; X-ray diffraction

1. Introduction

In the course of our ongoing research in ferrocenyl-substituted N-heterocycles [1] we focused our interest on the pyridazine derivatives. For many years considerable attention has been paid to the chemistry and biological activity of pyridazines [2–9]. It has been shown, e.g., that 1,3- and 1,4-*bis*[pyridazin-3(2*H*)-one-6-yl]benzenes, 4,4′-*bis*[pyridazin-3(2H)-one-6-yl]biphenyl and 2,5-*bis*[pyridazin-3(2*H*)-one-6-yl]thiophene and some of their partly saturated derivatives display generally stronger phosphodiesterase (PDE-III) inhibition than the corresponding *mono*-pyridazinone and this enhanced biological activity originates from the closer to optimal separation of two interacting polar heterocyclic moieties [5]. On the other hand, numerous ferrocene-containing heterocycles have also proved to be of pharmacological and even therapeutical interest [10–18]. In this context it seemed reasonable to convert the commercially available acetylferrocene and 1,1′-diacetylferrocene (**1** and **4**; Schemes 1 and 2) into 1-[pyridazin-3(2*H*)-one-6-yl]ferrocene (**3**) and 1,1′-*bis*-[pyridazin-3(2*H*)-one-6-yl]ferrocene (**5**), respectively. The presence of the easily transformable lactame moieties in **5** prompted us to undertake the preparation of a series of novel macrocyclic ferrocenophanes with interesting structures incorporating two heterocyclic units (Scheme 2).

☆ See Ref. [1].

* Corresponding author. Tel.: +36 1 209 0555; fax: +36 1 372 2592.
E-mail address: sohar@para.chem.elte.hu (P. Sohár).

0022-328X/$ - see front matter © 2004 Elsevier B.V. All rights reserved.
doi:10.1016/j.jorganchem.2004.09.086

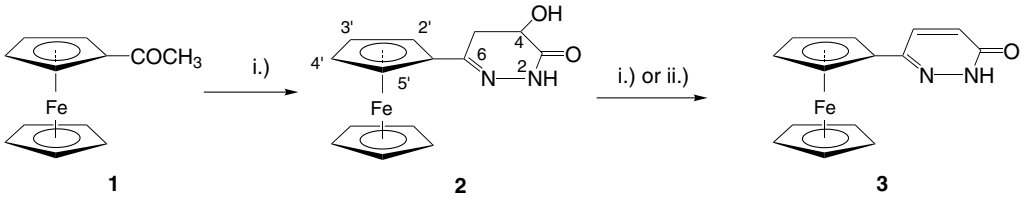

i.) OHC-COOH.H_2O / AcOH, 110 °C, then NH_4OH to pH = 8 and $N_2H_4.H_2O$ reflux.
ii.) $EtOH^-$ AcOH (2:1), reflux.

Scheme 1.

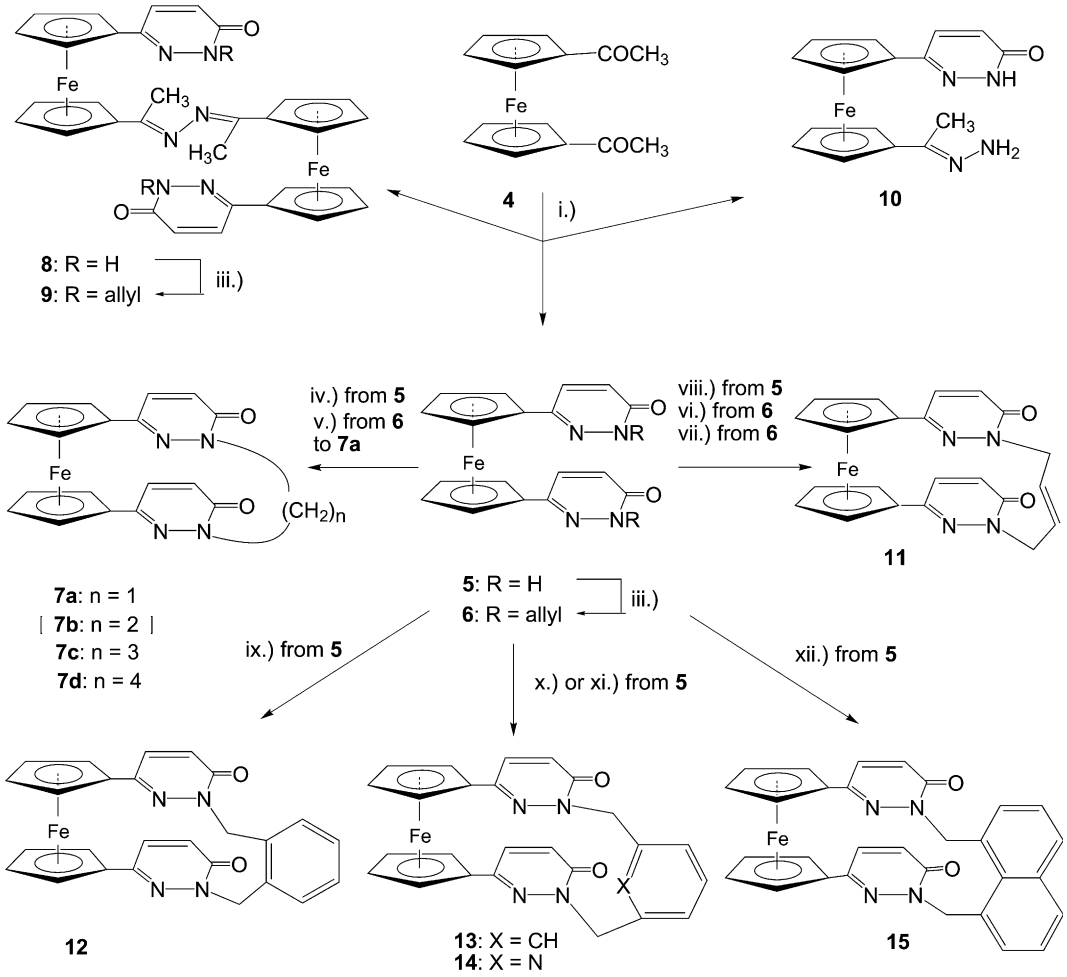

i.) OHC-COOH.H_2O / AcOH, 110 °C, then NH_4OH to pH = 8 and $N_2H_4.H_2O$ reflux.
iii.) CH_2=CH-CH_2Br, Bu_4NOH / CH_2Cl_2-MeOH (20:1), rt.
iv.) Br-$(CH_2)_n$-Br, Bu_4NOH / CH_2Cl_2-MeOH (20:1), reflux.
v.) $Cl_2RuP(C_6H_{11})_3$(=CH-Ph)(1,3-dimesitylimidazol-2-ylene)/ CH_2Cl_2, reflux.
vi.) $Cl_2RuP(C_6H_{11})_3$(=CH-Ph)(1,3-dimesitylimidazol-2-ylene)/ CH_2Cl_2 distilled from CaH_2, reflux.
vii.) $Cl_2RuP(C_6H_{11})_3$(=CH-Ph)(1,3-dimesitylimidazol-2-ylene)/ benzene, reflux.
viii.) (*E*)-(2)-$BrCH_2$-CH=CH-CH_2Br, Bu_4NOH / CH_2Cl_2-MeOH (20:1), rt.
ix.) *o*-$(BrCH_2)_2C_6H_4$, Bu_4NOH / CH_2Cl_2-MeOH (20:1), rt.
x.) *m*-$(BrCH_2)_2C_6H_4$, Bu_4NOH / CH_2Cl_2-MeOH (20:1), rt.
xi.) 2,6-$(BrCH_2)_2C_5H_3N$, Bu_4NOH / CH_2Cl_2-MeOH (20:1), rt.
xii.) 1,8-$(BrCH_2)_2C_{10}H_6$, Bu_4NOH / CH_2Cl_2-MeOH (20:1), rt.

Scheme 2.

2. Results and discussion

For the transformation of **1** and **4** into the corresponding pyridazinones we applied well-documented protocols [2,5,6] involving acid or base-catalyzed aldol addition of alkyl-aryl-ketones and glyoxylic acid followed by ring-closure with hydrazine. Under basic conditions (KOH/H_2O, K_2CO_3/H_2O) neither **1** nor **4** reacted with glyoxylic acid and they were recovered almost quantitatively from the reaction mixtures. However, by employing acetic acid as solvent for the crucial aldolisation both ferrocene-containing precursors could be transformed into the separable mixture of pyridazinone derivatives (**2**, **3**; Scheme 1, and **5**, **8**, **10**; Scheme 2) in moderate yields (15–55%). On treatment with a 2:1 mixture of ethanol and acetic acid dehydratation of **2** took place very easily yielding pyridazinone **3** (yield: 93%). Although, the reaction of **4** was conducted under the same conditions applied to the conversion of **1** we could not isolate 4-hydroxypyridazinone derivatives analogous to **2**. Instead, the dominant formation of azine **8** refers to the sluggish aldolisation of the second acetyl group inside the molecule. The unstable hydrazone **10** could be isolated in analytically pure form only in low yield (15%) because in the course of chromatography and crystallization it undergoes partial decomposition to black tarry substances. With a larger excess of glyoxylic acid in the reaction mixture the proportion of the desired *bis*-pyridazinone **5** slightly increased relative to **8** and **10**, however, the overall yield was much lower probably due to uncontrolled decomposition pathways.

By means of *N*-alkylation with bifunctional alkylating agents and *N*-allylation followed by ring closing metathesis (RCM) reaction [19] several attempts were made for cyclization of **5** and **8**, respectively, to obtain novel ferrocenophanes incorporating two pyridazinone rings separated by different bridging units. The alkylation reactions were conducted under phase-transfer conditions employing tetrabutylammonium hydroxide as base dissolved in a 20:1 mixture of CH_2Cl_2–MeOH. Dialkylation reactions of **5** with 1,3-dibromopropane and 1,4-dibromobutane carried out in dilute solutions (0.024 M) afforded the expected propylene- and butylene-bridged compounds **7c** and **7d**, respectively, in reasonable yields (46% and 35%). However, besides **7d** the methylene-bridged derivative **7a** could also be isolated in a moderate yield (18%), and the latter was the exclusively isolated product (yield: 40%) when the cyclization was attempted with 1,2-dibromoethane. In the absence of the reagent **7a** was obtained in 63% yield. Since the bridging element in **7a** was obviously originating from the solvent as reported also for other cases [20], dichloromethane was replaced by chloroform. Using this modified solvent mixture ($CHCl_3$–MeOH 20:1) the yields for **7c** and **d** became lower (25% and 19%, respectively), and the preparation of the desired ethylene-bridged **7b** failed again, only some decompositions resulting in black tarry substances were observed. It seems that 1,2-dibromoethane acts as a bromine-equivalent reagent which oxidizes the ferrocene unit carrying anionic substituent(s) under the applied basic conditions. Further attempts with other 1,2-disubstituted ethanes for the preparation of ferrocenophane **7b** are in progress.

Under the same phase-transfer conditions each attempt to perform analogous transformations of *bis*-ferrocene derivative **8** has not been successful so far, but uncontrolled polymerisation and/or decomposition took place in both the solvent mixtures used.

Another possibility for cyclisation of **5** and **8** was *N*-allylation on the two pyridazinone moieties followed by RCM. However, bridging of diallyl derivatives **6** and **9** (Scheme 2) could not be achieved by the commercial first generation Grubbs' catalyst [$Cl_2Ru(PCy_3)_2$=CHPh] dissolved in dichloromethane or benzene. In **9** an interesting double π-stacking interaction involving the two allylpyridazinone units and the azine moiety was detected by X-ray analysis (Fig. 1) which can be responsible for its decreased tendency to undergo intramolecular cyclisation.

We carried out further RCM experiments using second generation Grubbs' catalyst [$Cl_2Ru(PCy_3)$(=CHPh)(1,3-dimesitylimidazol-2-ylene)] for bridging **6** and **9**. As expected from the aforementioned structure of **9**, the reaction carried out in dichloromethane and benzene resulted in only polymer-like substances. Interestingly, when **6** was treated with this catalyst (10 mol%) in refluxing dichloromethane desallylation of both pyridazine rings followed by dialkylation with a solvent molecule afforded **7a** (yield: 38%). Analogous *N*-desallylations taking place by ruthenium-catalyzed isomerization followed by the hydrolysis of the enamine

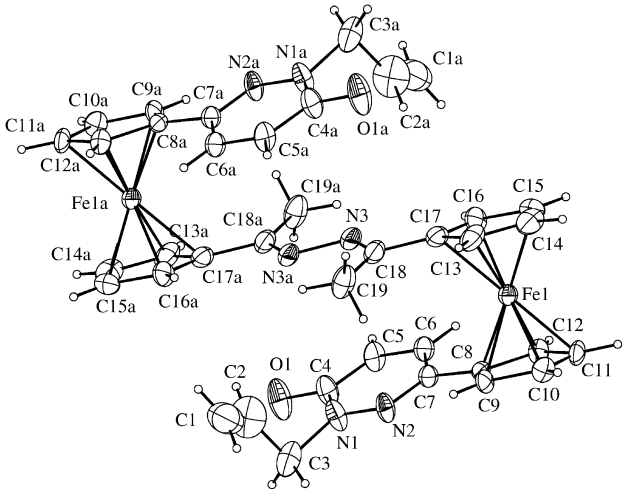

Fig. 1. X-ray structure of compound **9**

intermediate have recently been reported by Alcaide et al. [21]. When the catalytic reaction was conducted in anhydrous dichloromethane freshly distilled from CaH_2 and benzene, respectively, **6** underwent the expected RCM process leading to **11** containing the bridging C=C bond with *E*-configuration (Scheme 2). This configuration was proven preparatively: **11** was also obtained from **5** with (*E*)-1,4-dibromo-2-butene under phase-transfer conditions (Bu_4NOH/CH_2Cl_2–MeOH 20:1). Further bridged derivatives (**12**–**15**) were obtained from **5** by analogous phase-transfer alkylation with α,α′-dibromo-*o*-xylene, α,α′-dibromo-*m*-xylene, 2,6-*bis* (bromomethyl)pyridine and 1,8-*bis* (bromomethyl) naphthalene in excellent yields (92%, 76%, 80% and

Table 1
Characteristic IR frequencies [cm^{-1}] of compounds **2**, **3**, **5**, **6**, **7a,c,d** and **8**–**15** (in KBr discs)

Compound	*v*NH band (broad or diffuse)	Amide-I band	*v*C=N band	γ(=CH) band	ν_{as} Cp–Fe–Cp and tilt of Cp
2	3500–3000[a]	1677		1130[b]	488
3	3200–2200	1652, 1672	1587	814, 840	484, 498, 523
5	3250–2500	1662, 1681	1591	838	490, 528
6	–	1673	1599	809, 838	491
7a	–	1672, 1660	1593	839	521, 496
7c	–	1668	1591	844	478, 492, 511
7d	–	1663	1595	832, 841	518
8	3250–2500	1673, 1654	1591	837	485, 514
9	–	1664	1592	819, 856	464, 483
10	3400, 3500–2500	1677	1591	841, 817	490, 509, 528
11	–	1655	1590	833	492, 506, 519
12	–	1662	1591	843	502, 551
13	–	1655	1592	838	508, 539
14	–	1666	1592	840	493, 543
15	–	1667	1590	837	494, 506

[a] Coalesced with the *v*OH band.
[b] *v*C–O band.

Table 2
^{1}H NMR data[a] of compounds **2**, **3**, **5**, **6**, **7a,c,d** and **8**–**15**[b]

Compound	CH_3[c] *s* (3H)	NCH_2 (2H)[d]	H-5 *d* (1H)[e]	H-6 *d*(1H)	H2′,5′(2H)	H-3′,4′(2H)	NH *s*(1H)
					substituted *Cp* ring		
2	–		2.78, 2.98	4.10[f]	4.62	4.39	10.66
3	–	–	7.71	6.87	4.79	4.42	12.78
5	–	–	7.38	6.61	4.70	4.31	12.70
6	–	4.65	7.14	6.78	4.58	4.30	–
7a	–	6.27	7.83	7.04	4.62	4.44	–
7c	2.50	4.20	7.31	6.62	4.81	4.48	–
7d	1.58	4.04	7.70	6.93	4.55	4.52	–
8	1.90	–	7.64	6.83	4.71[g], 4.85	4.37[g], 4.47	12.81
9	1.89	4.62	7.66	6.88	4.84[g], 4.68	4.47[g], 4.38	–
10	1.76	–	7.57	6.83	4.73[g], 4.42	4.37[g], 4.18	12.77
11	–	~4.59	7.68	6.92	4.45	4.44	–
12	–	~5.35	6.86	6.65	4.36	4.26	–
13	–	5.15	7.84	6.98	4.60	4.57	–
14	–	5.15	7.56	6.71	4.64	4.39	–
15	–	~5.27, ~6.3	6.92	6.62	3.77, 4.44	4.11, 4.19	–

Further signals, OH (**2**): 5.52 (1H), *d* (*J*: 4.4.); H-1″-5″(unsubstituted *Cp* ring, 5H) 4.25 (**2**), 4.12 (**3**); allylic group, =CH: 5.95 m (1H) for **6** and **9**, $=CH_2$: 5.20 *d* (*J*: 11.2) and 5.21 *d* (*J*: 16.0) for **6** and 5.12 *dd* (*J*: 17.2, 1.5) and 5.17 *dd* (*J*: 10.3, 1.5) for **9**, respectively; NH_2 (**10**): 5.85 *s* (2H); =CH (**11**, olefinic group): 5.66 *m* (2H); ArH: 7.45 (**12**), ~*s* (4H), H-2: 6.67, ~*s* (**13**), H-4,6: 7.32 (**13**), 7.25 (**14**) ~*d* (2H), H-5: 7.37 (**13**), *dd* (1H) and 7.71 *t* (*J*: 7.7, **14**); naphthalene in **15**: H-γ: 7.48 *dd* (*J*: 7.0 and 1.5), H-δ: 7.53 *t*, H-ε: 8.03 *dd* (*J*: 8.0 and 1.5).

[a] In DMSO-d_6 solution ($CDCl_3$ for **6** and **12**, 5:1 mixture of $CDCl_3$ and CD_3OD for **15**) at 500 MHz. Chemical shifts in ppm (δ_{TMS} = 0 ppm), coupling constants in Hz.
[b] Assignments were supported by HMQC and HMBC (except for **5, 7c,d, 8, 11** and **12**) measurements and also 2D-COSY (for **7c**), respectively.
[c] Internal methylene group *m*, 2H (**7c**), 4H (**7d**).
[d] Doublet, *J*: 5.8 (4H, **6**), 5.5 (**9**), singlet (**7a**), broad, 4H (**7c,d, 11** and **12**), 2 × 2H (**15**).
[e] *J*: 9.7 ±0.2, 9.3 (**12**), 2 × *dd* (2H, methylene) for **2**: 2.78 (*J*: 16.8 and 9.4) and 2.98 (*J*: 16.8 and 6.2), respectively.
[f] Singlet-like signal (multiplet with coalesced lines).
[g] Pyridazine-substituted Cp ring.

86%). Analogous transformations of azine **8** neither in (*E*)-1,4-dibromobutene nor with the applied *bis*(bromomethyl)arenes have been succesful so far. Experiments with modified conditions and reagents are in progress.

The structures of the new compounds (**2**, **3**, **5**, **6**, **7a**,**c**,**d** and **8**–**15**) were determined by ^{1}H and ^{13}C NMR spectroscopy. The spectral data (Tables 1–3) are self-explanatory. Only a few additional remarks are necessary.

The chemical equivalence of the atomic pairs H/C-2′,5′ and H/C-3′,4′ in the cyclopentadienyl rings of **7a**,**c**,**d** and **11**–**14** suggests a free libration resulting in a quasi-symmetry of the chain binding the two nitrogens. For **2**, **3**, **5** and **6**, this chemical equivalence may arise from a free rotation around the C–C bond binding the hetero-ring to the cyclopentadienyl ring. In case of differently substituted cyclopentadienyl rings incorporated in **8**–**10**, of course, their signals appear separated both in the ^{1}H and ^{13}C NMR spectra but the above mentioned equivalence of the atomic pairs in all the cyclopentadienyl rings refers to free rotation of perpendicular cyclopentadienyl- and hetero rings or azine chain containing quasi-rigid structure. This fact suggests that the conformation of **9** is phase-dependent and the solid structure changes to a more flexible one in solution.

The resolved H/C-2′,5′ and H/C-3′,4′ signals of **15** confirms its rigid structure with the bulky naphthalene-containing bridging element of which libration seems to be unfavourable due to steric reasons.

Table 4
Selected bond lengths (Å), angles (°) and torsion angles (°) for **9**

Bond lengths		*Angles*	
C(1)–C(2)	1.29(2)	C(1)–C(2)–C(3)	123.4(17)
C(3)–C(2)	1.39(2)	C(2)–C(3)–N(1)	98.6(11)
N(1)–C(3)	1.55(1)		
C(19)–C(18)	1.50(1)	*Torsion angles*	
N(3)–C(18)	1.28(1)	N(1)–C(3)–C(2)–C(1)	−130.6(15)
N(3)–N(3)#1[a]	1.44(1)	C(16)–C(17)–C(18)–N(3)	−13.0(14)
		C(16)–C(17)–C(18)–C(19)	166.6(9)
		N(3)#1–N(3)–C(18)–C(17)[a]	179.7(8)
		N(3)#1–N(3)–C(18)–C(19)[a]	0.1(15)

[a] Symmetry transformations used to generate equivalent atoms: #1: $-x, -y+1, -z$.

The presence of the stereogenic centre at C-4 in **2** leads to chemical non-equivalence of C-2′ and C-5′ and also C-3′ and C-4′ atom pairs, resp., and as a consequence their lines are separated.

The H/C-5 and H/C-6 signals, and to a lesser extent, the H/C-2′,5′ and H/C-3′,4′ signals are also upfield shifted for **12**, perhaps as a consequence of a bent conformation involving a concave molecular skeleton in which the anisotropic shielding (in ^{1}H NMR) and a steric interaction (in ^{13}C NMR), resp., can explain the observed upfield shifts.

It is noteworthy, that the usual polarisation of enones causing a large difference in the ^{1}H and ^{13}C NMR shifts of α- and β-H/C atoms is absent in our pyridazinones due to extension of the conjugated system to the C=N

Table 3
^{13}C NMR chemical shifts[a] of compounds **2,3,5,6,7a,c, d** and **8–15**[b,c]

Compound	Pyridazine ring				Substituted *Cp* ring			NR group[d]			
	C-3	C-4	C-5	C-6	C1′	C-2′,5′	C-3′,4′	C-α	C-β	C-γ	C-δ
2	168.6	63.5	33.2	152.1	82.2	67.1, 67.5[e]	70.6, 70.7[e]	–	–	–	
3	161.0	130.2	133.2	146.3	81.1	67.3	70.7	–	–	–	–
5	160.8	129.9	132.7	144.8	82.4	68.3	71.7	–	–	–	–
6	159.6	129.7	130.7	145.2	81.6	68.3	71.8	54.7	132.3	118.9	–
7a	162.0	129.6	131.9	145.5	82.6	70.1	71.7	63.1	–	–	–
7c	159.5	129.6	131.3	141.8	82.1	68.1	71.2	51.7	23.5	–	–
7d	160.2	129.5	131.3	145.5	81.8	69.5	71.4	47.1	24.6	–	–
8	161.1	130.3	133.0	145.4	82.3[f], 85.6	68.2[f], 69.2	71.7, 71.8	–	–	–	–
9	159.4	129.8	132.3	145.5	82.0[f], 85.6	68.4[f], 69.4	71.75[f], 71.80	54.0	133.6	118.3	
10	161.1	130.0	133.1	145.8	81.8[f], 88.7	67.6, 67.9[f]	70.4, 71.2[f]	–	–	–	–
11	159.4	129.9	131.6	145.9	82.1	69.5	71.1	50.2	130.2	–	–
12	159.2	129.1	129.4	141.9	81.9	67.3	70.6	52.8	135.5[g]	133.7	128.6
13	159.2	130.3	131.6	145.8	82.3	69.5	71.4	54.9	138.9[g]	127.9	129.2[h]
14	159.4	129.5	132.8	143.9	83.3	68.4	70.9	56.7	155.7[g]	121.4	137.8[h]
15	160.5	128.3	129.7	142.6	81.3	66.7, 67.4[e]	70.3, 71.0	55.8	135.8[g]	133.6[i]	129.8[i]

[a] In DMSO-d_6 solution ($CDCl_3$ for **6** and **12**, 5:1 mixture of $CDCl_3$ and CD_3OD for **15**) at 125 MHz. Chemical shifts in ppm ($\delta_{TMS} = 0$ ppm).
[b] Assignments were supported by DEPT (except for **7c**), HMQC and for **2, 3, 6, 7a, 9, 10** and **13–15** also by HMBC measurements.
[c] Further signals: C1″-5″(unsubstituted Cp ring): 69.9 (**2**), 70.1 (**3**); CH_3: 16.1 (**8** and **9**), 13.2 (**10**); C=N (chain): 158.5 (**8** and **9**), 142.7 (**10**); C-2 (benzene ring): 122.9 (**13**).
[d] Side chain or bridging group.
[e] Line separation is due to presence of a chiral carbon (**2**) or rigid; non-symmetric conformation (**15**).
[f] Pyridazine–substituted *Cp* ring.
[g] Substituted aromatic carbon.
[h] C-4.
[i] Anellational carbon of naphthalene in **15** (C-γ and C-δ). CH-carbons of naphthalene in **15**: C-γ′: 135.3, C-δ′: 125.2, C-ε: 131.5.

bond of which N atom – having electron reservoir character – equalises the high difference in electron density around the carbon atoms in question. For the same reason, the carbonyl is more shielded (its line appears in the interval of 159.2–162.0 ppm) than in "normal" amides generally (as also in case of **2**, where the C=O line appears at 168.6 ppm).

X-ray analysis of **9** revealed the above mentioned double π-stacking interaction (Fig. 1). The selected bond parameters are listed in Table 4. The molecule has a symmetry centre at the middle of the N3–N3a bond. The coplanar azine moiety including the symmetry centre has an angle of 11.5(7)° to the Cp ring. The angle between the pyridazone ring and the Cp ring is 18.2(5)°. The planar angle of the two Cp rings having a staggered conformation in both ferrocenyl moieties is 1.0(7)°, with Fe atom being 1.640(4) Å from each of them.

3. Conclusion

By means of a previously described one-pot procedure the commercially available 1,1′-diacetylferrocene **4** can easily be converted into 1,1′-*bis*-[pyridazin-3(2H)-one-6-yl]ferrocene (**5**), which is an easily transformable precursor in a wide range of coupling reactions. The reported facile bridging reactions carried out by phase-transfer alkylations and RCM protocol may open up convenient ways for the preparation of a large variety of novel ferrocenophanes also incorporating differently separated aromatic/heteroaromatic rings. Certain macrocyclic ferrocenophanes with nitrogen-containing bridging elements (e.g., pyridine in **14** and its possible bipyridyl, phenanthridyl, etc., analogues) which can be obtained by phase-transfer alkylations may also be applied in homogenous catalysis as polydentate ligands.

4. Experimental

Melting points (uncorrected) were determined with a Boetius microstage. IR spectra were recorded in KBr pellets with a BRUKER IFS 55 FT-spectrometer. ^{1}H and ^{13}C NMR spectra were recorded in $CDCl_3$ and DMSO-d_6 solution in 5 mm tubes at RT, on a Bruker DRX 500 spectrometer at 500 (^{1}H) and 125 (^{13}C) MHz, resp. with the deuterium signal of the solvent as the lock and TMS as internal reference. The standard Bruker microprogram NOEMULT.AU to generate NOE was used with a selective preirradiation time. DEPT spectra were run in a standard manner, using only the $\Theta = 135°$ pulse to separate CH/CH_3 and CH_2 lines phased "up" and "down", respectively. 2D-HMQC and 2D-HMBC spectra were obtained by using the standard Bruker pulse programs INV4GS and INV4GSLPLRND, respectively.

A red needle crystal of **9** having approximate dimensions of $0.22 \times 0.12 \times 0.42$ mm was mounted on a glass fiber. All measurements were made on a Rigaku AFC6S diffractometer with graphite monochromated Cu Kα radiation ($\lambda = 1.5418$ Å).

Cell constants and an orientation matrix for data collection were obtained from a least-squares refinement using carefully centered reflections in the range $20.16° < 2\theta < 24.43°$.

The data were collected at a temperature of 293 K using the $\omega - 2\theta$ scan technique to a maximum 2θ value of 150.2°. Of the 11 724 reflections, which were collected, 5433 were unique. The intensities of three representative reflections were measured after every 150 reflections. The linear absorption coefficient, μ, for Cu Kα radiation is 7.392 mm^{-1}. An empirical absorption correction based on azimuthal scans of several reflections was applied which resulted in transmission factors ranging from 0.76 to 1.00.

Data processing was carried out using the software supplied with the diffractometer. The crystal data were as follows: $C_{38}H_{36}Fe_2N_6O_2$, $M_w = 720.43$, triclinic space group $P\bar{1}$, $a = 9.446(5)$ Å, $b = 9.844(2)$ Å, $c = 17.955(8)$ Å, $\alpha = 90.12(3)°$, $\beta = 98.09(5)°$, $\gamma = 89.92(3)°$, $V = 1652.8(12)$ $Å^3$, $Z = 2$, $D_c = 1.448$ g cm^{-3}. Structure solution with direct methods was carried out with the teXsan package [22] using default parameters. The refinement was carried out by using the SHELXL-97 [23] program with the full-matrix least-squares method on F^2. All non-hydrogen atoms were refined anisotropically. Hydrogen atoms were generated and refined by the riding model. The refinement converged to $R = 0.0692$, $wR = 0.1182$ for 1795 ($I > 2\sigma I$) reflections. The maximum and minimum peaks on the final Fourier map were 0.278 and −0.402 e $Å^3$, respectively.

Crystallographic data for the structural analysis has been deposited with the Cambridge Crystallographic Data Centre, CCDC No. 223618 for compound **9**.

4.1. General procedure for the synthesis of pyridazinones from acetylferrocene (1) and 1,1′-diacetylferrocene (4)

The mixture of acetylferrocene (5.69 g, 25 mmol)/1,1′-diacetylferrocene (3.38 g, 12.5 mmol) and glyoxylic acid-hydrate (2.35 g, 25 mmol) was stirred in AcOH (4 mL) at 105 °C under argon for 3 h. After cooling to r.t., water (10 mL) was added to the deep red mixture. Meanwhile cooling with ice-water the pH was set to 8 with conc. NH_4OH solution and the unreacted ketone was filtered off. Following the extraction with EtOAc (5×12 mL), hydrazine-hydrate (1.25 mL) was added to the aqueous solution which was then heated under reflux for 4 h. After cooling, the precipitated brown powder was purified by flash column chromatography on silica with CH_2Cl_2–MeOH (10:1) to separate the mixture

of the products which were further purified by crystallisation from ethanol.

4.2. [4-Hydroxy-4,5-dihydropyridazin-3(2H)-one-6-yl]ferrocene (**2**)

Yellowish-brown powder, yield 2.76 g (37%), m.p. 194–196 °C. Anal. Found: C, 56.50; H, 4.77; N 9.45. Calc. for $C_{14}H_{14}FeN_2O_2$: C, 56.41; H, 4.73; N, 9.40%.

4.3. [Pyridazin-3(2H)-one-6-yl]ferrocene (**3**)

Deep orange powder, yield 3.85 g (55%), m.p. 207–210 °C. Anal. Found: C, 59.96; H, 4.30; N, 9.95. Calc. for $C_{14}H_{12}FeN_2O$: C, 60.03; H, 4.32; N, 10.00%.

4.4. 1,1′-Bis-[pyridazin-3(2H)-one-6-yl]ferrocene (**5**)

Orange powder, yield 1.31 g (28%), m.p. 293–297 °C. Anal. Found: C, 57.76; H, 3.80; N, 14.89. Calc. for $C_{18}H_{14}FeN_4O_2$: C, 57.78; H, 3.77; N, 14.97%.

4.5. N,N′-Bis-1-[1′-[pyridazin-3(2H)-one-6-yl]ferrocene-1-yl]ethylidenehydrazine (**8**)

Orange powder, yield 1.40 g (35%), m.p. 282–285 °C. Anal. Found: C, 60.11; H, 4.35; N, 13.21. Calc. for $C_{32}H_{28}Fe_2N_6O_2$: C, 60.02; H, 4.41; N, 13.13%.

4.6. N-1-[1′-[Pyridazin-3(2H)-one-6-yl]ferrocene-1-yl] ethylidenehydrazine (**10**)

Brownish powder, yield 0.64 g (15%), m.p. 291–297 °C (decomp.). Anal. Found: C, 56.94; H, 4.98; N,16.67. Calc. for $C_{16}H_{16}FeN_4O$: C, 57.17; H, 4.80; N, 16.67%.

4.7. Acid-catalysed dehydration of **2**

A solution of 0.30 g (1 mmol) of **2**, ethanol (4 mL) and glacial acetic acid (2 mL) was heated under reflux for 10 min then evaporated to dryness. The solid residue was triturated with ethanol and filtered off to obtain **3** in analytically pure form: 0.26 g (93%).

4.8. General procedure for phase-transfer dialkylation reactions of bis-pyridazinones **5** and **8**

The corresponding *bis*-pyridazinone **5/8** (1 mmol) was suspended in CH_2Cl_2 (40 mL) under argon. To this suspension 1 M methanolic solution of Bu_4NOH (2 mL) was added and stirred for 5 min. After this period 0.242 g (2 mmol) of allylbromide or 1 mmol of the corresponding dibromo compound was added and the resulting solution was heated under reflux (with α,ω-dibromoalkanes) or stirred at room temperature [with allylbromide, (*E*)-1,4-dibromo-2-butene, α,α′-dibromo-*o*-xylene, α,α′-dibromo-*m*-xylene, 2,6-*bis*(bromomethyl) pyridine and 1,8-*bis*(bromomethyl)-naphthalene] for 3 h. The basic solution of **5** was heated under reflux for 3 h also in the absence of dibromo reagents. After evaporation of the reaction mixture, the residue was purified by flash column chromatography on silica with CH_2Cl_2–MeOH (10:1) to obtain the product as the first eluting deep red band which – except for the highly soluble diallyl compound **6** – was further purified by crystallization with ethanol. Using $CHCl_3$ (40 mL) instead of CH_2Cl_2 the analogous procedure was also carried out for the reactions of **5** with 1,3-dibromopropane and 1,4-dibromobutane, respectively.

4.9. Conversions of **6** effected by [1,3-bis-(2,4,6-trimethylphenyl)-2-imidazolidinylidene-dichloro-(phenylmethylene)-tricyclohexylphosphine]ruthenium (second generation Grubbs' catalyst)

The mixture of **6** (0.454 g, 1 mmol) and the catalyst (0.085 g, 0.1 mmol) was dissolved in the corresponding solvent (80 mL of freshly distilled benzene or CH_2Cl_2 distilled in the absence or in the presence of CaH_2). The red solution obtained was heated under reflux under argon for 8 h, then the solvent was evaporated. The residue was twice purified by flash column chromatography on silica with $CHCl_3$ to obtain the product as the first eluting band (**7a**: $R_f = 0.48$, **11**: $R_f = 0.43$) which was further purified by crystallisation with ethanol. The collection and evaporation of the second band ($R_f = 0.35$) recovered the unchanged precursor **6** [0.12 g (26%) after the reaction conducted in benzene; 0.20 g (45%) after the reaction conducted in CH_2Cl_2; 0.27 g (61%) after the reaction carried out in CH_2Cl_2 freshly distilled from CaH_2].

4.10. 1,1′-Bis-[2-allylpyridazin-3(2H)-one-6-yl] ferrocene (**6**)

Orange oil, yield 0.37 g (81%). Anal. Found: C, 63.40; H, 4.81; N,12.4. Calc. for $C_{24}H_{22}FeN_4O_2$: C, 63.45; H, 4.88; N, 12.33%.

4.11. Bis-[6,6-(ferrocene-1,1′-diyl)-2,2-methylene] pyridazin-3(2H)-one (**7a**)

Deep red powder, yield 0.16 g (40%) from the reaction conducted in the presence of 1,2-dibromoethane; 0.07 g (18%) from the reaction conducted in the presence of 1,4-dibromobutane; 0.25 g (63%) from the reaction conducted in the absence of dibromoalkane; 0.15 g (38%) by RCM procedure conducted in CH_2Cl_2 contaminated with water, m.p. 202–203 °C. Anal. Found: C, 59.14; H, 3.60; N, 14.4. Calc. for $C_{19}H_{14}FeN_4O_2$: C, 59.09; H, 3.65; N, 14.51%. MS (FAB) Found: *m/z* 386. Calc. 386.

*4.12. Bis-[6,6-(ferrocene-1,1′-diyl)-2,2-propylene]pyridazin-3(2H)-one (**7c**)*

Orange powder, yield 0.19 g (46%) from the reaction conducted in CH_2Cl_2–MeOH (20:1); 0.11 g (25%) from the reaction conducted in $CHCl_3$–MeOH (20:1), m.p. 154–157 °C. Anal. Found C, 60.92; H, 4.46; N, 13.50. Calc. for $C_{21}H_{18}FeN_4O_2$: C, 60.90; H, 4.38; N, 13.53%. MS (FAB) Found: *m/z* 414. Calc. 414.

*4.13. Bis-[6,6-(ferrocene-1,1′-diyl)-2,2-butylene]pyridazin-3(2H)-one (**7d**)*

Orange powder, yield 0.15 g (35%) from the reaction conducted in CH_2Cl_2–MeOH (20:1); 0.08 g (19%) from the reaction conducted in $CHCl_3$–MeOH (20:1), m.p. 133–135 °C. Anal. Found C, 61.77; H, 4.80; N, 12.98. Calc. for $C_{22}H_{20}FeN_4O_2$: C, 61.70; H, 4.71; N, 13.08%. MS (FAB) Found: *m/z* 428. Calc. 428.

*4.14. N,N′-Bis-1-[1′-[2-allylpyridazin-3(2H)-one-6-yl]ferroce-1-yl]ethylidenehydrazine (**9**)*

Brownish red cubes, yield 0.64 g (90%), m.p. 197–200 °C. Anal. Found C, 63.98; H, 5.12; N, 11.77. Calc. for $C_{38}H_{36}Fe_2N_6O_2$: C, 64.07; H, 5.09; N 11.80%.

*4.15. Bis-[6,6-(ferrocene-1,1′-diyl)-2,2-(E-but-2-en-1,4-diyl)]pyridazin-3(2H)-one (**11**)*

Yellow powder, yield: 0.37 g (87%) by phase-transfer alkylation; 0.19 g (44%) by RCM procedure carried out in CH_2Cl_2 freshly distilled from CaH_2; and 0.24 g (56%) by RCM procedure conducted in benzene, m.p. 128–131 °C. Anal. Found: C, 62.06; H, 4.26; N, 13.19. Calc. for $C_{22}H_{18}FeN_4O_2$: C, 61.99; H, 4.26; N, 13.14%. MS (FAB) Found: *m/z* 426. Calc. 426.

*4.16. Bis-[6,6-(ferrocene-1,1′-diyl)-2,2-(benzene-1,2-diyl)-methyl]pyridazin-3(2H)-one (**12**)*

Yellow powder, yield 0.44 g (92%), m.p. 145–147 °C. Anal. Found: C, 65.45; H, 4.29; N, 11. 84. Calc. for $C_{26}H_{20}FeN_4O_2$: C, 65.56; H, 4.23; N, 11.76%. MS (FAB) Found: *m/z* 476. Calc. 476.

*4.17. Bis-[6,6-(ferrocene-1,1′-diyl)-2,2-(benzene-1,3-diyl)-methyl]pyridazin-3(2H)-one (**13**)*

Yellow powder, yield 0.36 g (76%), m.p. 124–125 °C. Anal. Found: C, 65.60; H, 4.18; N, 11.77. Calc. for $C_{26}H_{20}FeN_4O_2$: C, 65.56; H, 4.23; N, 11.76%. MS (FAB) Found: *m/z* 476. Calc. 476.

*4.18. Bis-[6,6-(ferrocene-1,1′-diyl)-2,2-(pyridine-2,6-diyl)-methyl]pyridazin-3(2H)-one (**14**)*

Yellow powder, yield 0.38 g (80%), m.p. 128–130 °C. Anal. Found: C, 62.93; H, 3.95; N, 14.74. Calc. for $C_{25}H_{19}FeN_5O_2$: C, 62.91; H, 4.01; N, 14.67%. MS (FAB) Found: *m/z* 477. Calc. 477.

*4.19. Bis-[6,6-(ferrocene-1,1′-diyl)-2,2-(naphthalene-1,8-diyl)-methyl]pyridazin-3(2H)-one (**15**)*

Yellow powder, yield 0.45 g (86%), m.p. 233–234 °C. Anal. Found: C, 68.61; H, 4.12; N, 10.7. Calc. for $C_{30}H_{22}FeN_4O_2$: C, 68.46; H, 4.21; N, 10.64%. MS (FAB) Found: *m/z* 526. Calc. 526.

Acknowledgements

The authors thank the Hungarian Research Foundation (OTKA) for Grants T-043634 and TS-040732, and to the Hungarian-German Intergovernamental S&T Cooperation Programme (OMFB-WZT) for financial support D-35/99.

References

[1] Part 13 A. Csámpai, Gy. Túrós, V. Kudar, K. Simon, H. Oeynhausen, H. Wamhoff, P. Sohár, Eur. J. Org. Chem. 4 (2004) 717.
[2] G. Cignarella, D. Barlocco, G.A. Pinna, M. Loriga, M.M. Curzu, O. Tofanetti, M. Germini, P. Cazzulani, E. Cavalletti, J. Med. Chem. 32 (1989) 2277, and references therein.
[3] M. Tisler, B. Stanovnik, Adv. Heterocycl. Chem. 49 (1990) 385, and references therein.
[4] G. Heinisch, H. Kopelent, Prog. Med. Chem. 29 (1992) 141, and references therein.
[5] W.J. Coates, H.D. Prain, M.L. Reeves, B.H. Warrington, J. Med. Chem. 33 (1990) 1735, and references therein.
[6] W.J. Coates, A. McKillop, Synthesis (1993) 334, and references therein.
[7] P.G. Baraldi, A. Bigoni, B. Cacciari, C. Caldari, S. Manfredini, G. Spallutto, Synthesis (1991) 1158, and references therein.
[8] S. Moreau, P. Coudert, C. Rubat, D. Gardette, D. Valleegoyet, J. Couquelet, P. Bastide, P. Tronche, J. Med. Chem. 37 (1994) 2153, and references therein.
[9] P. Mátyus, J. Heterocycl. Chem. 35 (1998) 1075, and references therein.
[10] E.I. Edwards, R. Epton, G. Marr, J. Organomet. Chem. 168 (1979) 259, and references therein.
[11] K.E. Dombrowski, W. Baldwin, J.E. Sheats, J. Organomet. Chem. 302 (1986) 281.
[12] V. Scarcia, A. Furlani, B. Longato, B. Corain, G. Pilloni, Chim. Acta 67 (1988) 153.
[13] E.W. Neuse, M.G. Meirim, N.F. Blom, Organometallics 7 (1988) 2562.
[14] D.T. Hill, R.K. Johnson, P.D. Stupic, J.H. Zhang, W.M. Reiff, D.S. Egleston, Inorg. Chem. 28 (1989) 3529.
[15] A. Houlton, R.M.G. Roberts, J. Silver, J. Organomet. Chem. 107 (1991) 418.

[16] S. Top, J. Tang, A. Vessieres, D. Carrez, C. Prorot, G. Jaouen, Chem. Commun. (1996) 955.
[17] S. Top, A. Vessiéres, C. Cabestaing, I. Laios, G. Leclerq, C. Provot, G. Jaouen, J. Organomet. Chem. 637–63 (2001) 500.
[18] L. Delhaes, H. Abessolo, C. Biot, L. Berry, P. Delcourt, L. Maciejewski, D. Camus, D. Dive, J. Brocard. Parasitol. Res. 87 (2001) 239.
[19] (a) R.R. Schrock, J.S. Murdzek, G.C. Bazan, J. Robbins, M. DiMare, M. O'Regan, J. Am. Chem. Soc. 112 (1990) 3875, and references therein;
(b) R.H. Grubbs, S. Chang, Tetrahedron 54 (1998) 4413, and references therein;
(c) A review: A.J. Philips, A.D. Abell, Aldrichim. Acta 32 (1999) 75–88;
(d) J.L. Locke, C. Jones, C.J. Richards, J. Organomet. Chem. 637–639 (2001) 669;
(e) Gy. Túrós, A. Csámpai, T. Lovász, A. Györfi, H. Wamhoff, P. Sohár, Eur. J. Org. Chem. (2002) 3801, and references therein.
[20] (a) L.J. Powers, D.J. Eckert, L. Gehrlein, J. Pharm. Sci. 70 (1981) 419;
(b) S. Julia, P. Sala, J. Delmazo, M. Sancho, C. Ochoa, J. Elguero, J.P. Fayet, M.C. Verkut, J. Heterocycl. Chem. 19 (1982) 1141;
(c) R.M. Claramunt, H. Hernandez, J. Elguero, S. Julia, Bull. Chem. Soc. Fr. 2 (1983) 5.
[21] B. Alcaide, P. Almendros, J.M. Alonso, Chem. Eur. J. 9 (2003) 5793.
[22] teXsan for Windows version 1.06: Crystal Structure Analysis Package, Molecular Structure Corporation (1997–99).
[23] G.M. Sheldrick, SHELXL-97, Program for the Refinement of Crystal Structures, University of Göttingen, Germany, 1997.